

Looped Polarization-Insensitive Fiber Optical Parametric Amplifiers for Broadband High Gain Applications

Vladimir Gordienko , Filipe M. Ferreira , Senior Member, IEEE, Chandra B. Gaur , and Nick J. Doran

Abstract—We investigate polarization insensitive fiber optical parametric amplifiers (FOPAs) employing a balanced polarization diversity loop with at least two unidirectional gain fibers. We describe and compare three variants of looped polarization insensitive FOPAs optimized for noise figure, mitigation of nonlinear impairments and their trade-off, respectively. The test scenario consists of amplifying, by up to 14 dB, a set of 21×50 GHz-spaced channels including a 35 GBaud PDM-QPSK signal, and evaluating a power of nonlinear crosstalk, noise figure and amplified signal BER for each variant. For the first time we demonstrate a polarization insensitive FOPA amplifying WDM signals with a noise figure as low as 5.8 dB, and a polarization insensitive FOPA with output WDM signal power of 23 dBm. The testing results let us identify likely application scenarios for each looped FOPA variant. We justify potential implementation of polarization-insensitive FOPAs in future optical communication systems by arguing its ability to deliver low noise figure <6 dB for output signal power as high as 29 dBm and to enable polarization insensitive gain for the most prominent single-polarization FOPA achievements realizing ultrawide high gain.

Index Terms—Nonlinear optics, optical fiber amplifiers, optical fiber communication, optical parametric amplifiers, wavelength-division multiplexing.

I. INTRODUCTION

FIBER optical parametric amplifiers (FOPAs) have the potential to play an important role in future optical communications by surpassing limits associated with fiber-doped amplification. FOPA allows for an ultimate wavelength flexibility highly beneficial for emerging ultra-wideband optical communications [1]. Thus, FOPAs can operate in arbitrary wavelength

range [2], and its operation across O, E, S, C, and L bands and beyond has already been demonstrated [3]–[6]. In addition, FOPA can provide a virtually unconstrained gain bandwidth [2] with experimental demonstrations reaching 270 nm [7]. An exclusive ability of parametric amplifiers (including FOPA) is phase-sensitive amplification [8]. It allows for noise figure approaching 0 dB [9] and can double sensitivity (or capacity) of low SNR links [10] or significantly increase a fiber optic link reach, e.g., more than fivefold in [11]. FOPA stands out with its virtually instantaneous response time (~ 1 fs) [12]. It therefore allows for transient-free operation in ultra-fast applications and optical communication links with bursty traffic, where FOPA can have a significant advantage over doped-fiber and Raman amplifiers [13]. Although FOPAs share most of their merits with other optical parametric amplifiers (e.g., based on LiNbO_3) [14], [15], FOPAs are capable of much higher output signal power due to superior power handling of optical fiber.

Most of these FOPA achievements have been demonstrated using a single-polarization gain, but field applications require polarization insensitive (PI) gain, which is challenging to achieve with FOPA. A FOPA employing two orthogonally-polarized pumps has been shown to provide a PI gain up to 15 dB over a bandwidth up to 20 nm for a single channel [16]. However, WDM signals have only been amplified over bandwidth of 8 nm with on/off gain of 10 dB [17]. The key issues of PI-FOPAs are the three-fold gain coefficient reduction due to pumps orthogonality [18], and the requirement to have two high power pumps separated by bandwidth more than twice that of the WDM signals [6].

Instead, a polarization diversity loop with unidirectional gain fibers can greatly extend the potential of PI-FOPAs [19]. In this configuration an input signal is split into orthogonal linearly-polarized components counter-propagating in a loop (Fig. 1(a)–(c)). The signal components are independently but equally amplified within the loop before being recombined. The loop employs at least two gain fiber lengths each pumped unidirectionally and therefore amplifying only the signal component co-propagating with a pump. Consequently, each signal component passes through a ‘Gain’ section where it is amplified and a ‘Loss’ section where it has no gain but passive attenuation (Fig. 2). Employment of unidirectional gain sections in the loop prevents the detrimental nonlinear interaction between counter-propagating dithered pumps (due to Brillouin scattering

Manuscript received April 16, 2021; revised June 29, 2021; accepted July 16, 2021. Date of publication July 26, 2021; date of current version October 4, 2021. This work was supported in part by U.K. Engineering and Physical Sciences Research Council under Grants EP/R024057/1 (FPA-ROCS) and EP/M005283/1 (UPON) and in part by the UKRI Future Leaders Fellowship under Grant MR/T041218/1. (Corresponding author: Vladimir Gordienko.)

Vladimir Gordienko, Chandra B. Gaur, and Nick J. Doran are with the Institute of Photonics, Aston University, Birmingham B4 7ET, U.K. (e-mail: v.gordienko1@aston.ac.uk; gaurc@aston.ac.uk; n.j.doran@aston.ac.uk).

Filipe M. Ferreira was with the Institute of Photonics, Aston University, Birmingham B4 7ET, U.K. He is now with the University College London, London WC1E 6BT, U.K. (e-mail: filipef@ieee.org).

Color versions of one or more figures in this article are available at <https://doi.org/10.1109/JLT.2021.3099441>.

Digital Object Identifier 10.1109/JLT.2021.3099441

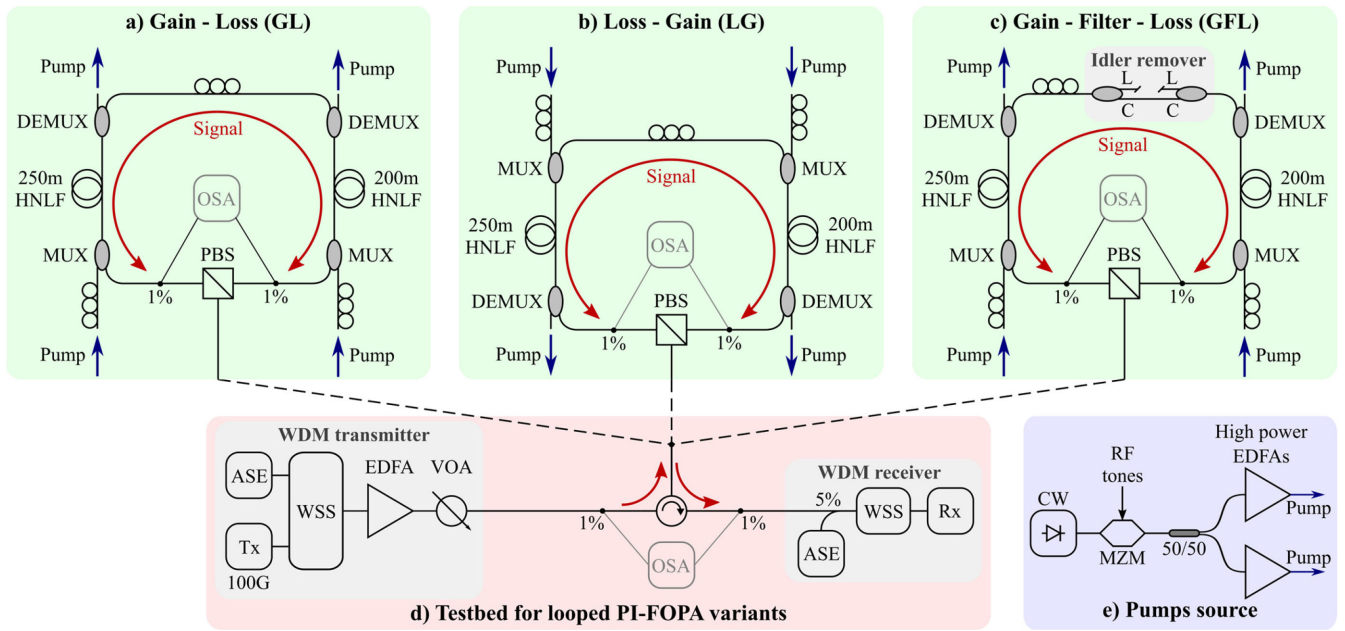


Fig. 1. Experimental setups of the three looped PI-FOPA variants (a)–(c), a testbed for their characterization (d), and a pump source used with all FOPA variants (e).

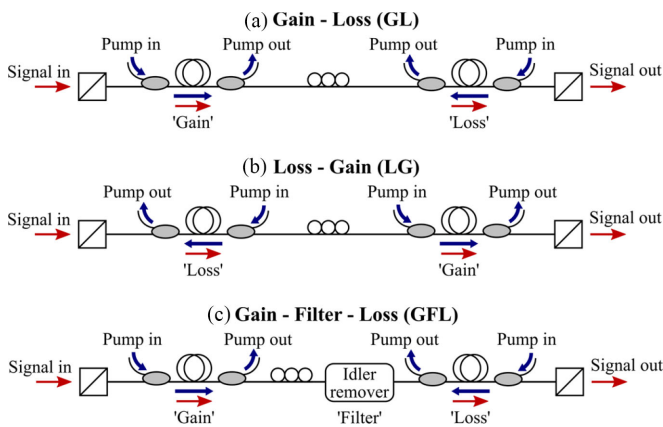


Fig. 2. A path of signal components in the loop for the three PI-FOPA variants. The signal path representation is the same for both signal components.

and four-wave mixing) occurring in the case of high bidirectional gain [20].

Looped PI-FOPAs have enabled dual-polarization WDM amplification with net gain up to 20 dB across bandwidth up to 18 nm [21] and the first-ever employment of FOPA in a recirculating loop for multi-span transmission [22]. Loop PI-FOPAs essentially consist of two or more single-polarization FOPAs so they have a great potential to inherit achievements of polarization-sensitive FOPAs both degenerate and non-degenerate (i. e. single- and dual-pump) and thus to deliver ultra-wide bandwidth high gain polarization-insensitive parametric amplification [6], [23].

The first looped PI-FOPA variant called “Gain – Loss” (GL) has each signal component first amplified in the respective ‘Gain’ section and then propagated through the respective ‘Loss’ section (Fig. 1(a), Fig. 2(a)) [19]. It allows for the best noise

figure according to the Friis formula [24] by minimizing signal loss preceding amplification [25]. However, the propagation of amplified signals through the ‘Loss’ section can lead to significant nonlinear impairments [21] and degrade the FOPA performance for broadband WDM applications.

Another variant of the looped PI-FOPA called “Loss – Gain” (LG) was proposed in [21] to mitigate nonlinear impairments by first propagating low power signal through the ‘Loss’ section and then amplifying it in the ‘Gain’ section (Fig. 1(b), Fig. 2(b)). The LG variant has indeed reduced the nonlinear impairments by 11.5 dB as compared to the GL variant [26]. However, it was unclear if this improvement outweighs a linear noise figure penalty envisaged for the LG variant due to placing the ‘Gain’ section after most of the loop insertion loss.

In this paper we propose a new looped PI-FOPA variant called “Gain – Filter – Loss” (GFL), and compare performance of all three variants (GL, LG and GFL) for applications in fiber optical communications. The GFL variant features a filter removing idlers between the ‘Gain’ and the ‘Loss’ sections (Fig. 1(c), Fig. 2(c)), which allows to eliminate inter-channel nonlinear impairments (nonlinear crosstalk) involving idlers in the ‘Loss’ section [27]. We employ each of three looped PI-FOPA variants to amplify a set of 21 WDM channels as their power is varied and evaluate nonlinear crosstalk power, noise figure and BER of a 35 GBaud PDM-QPSK channel. We demonstrate the GFL variant to mitigate nonlinear crosstalk power by up to 4.9 dB as compared to the GL variant without incurring a noise figure penalty. Although the LG variant provided a further nonlinear crosstalk mitigation by up to 12.1 dB, it suffered from ~ 6 dB noise figure penalty. Therefore, the proposed GFL variant allowed for the highest output signal power of a polarization insensitive FOPA with net gain of 14 dB and a noise figure of ~ 6 dB in a WDM environment demonstrated for the first time to

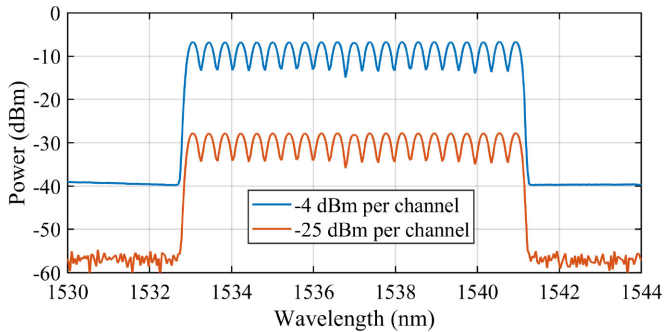


Fig. 3. Optical power spectra measured at the FOPA input show WDM channels at their highest (blue) and the lowest (red) power.

the best of our knowledge. Nevertheless, we suggest application scenarios for each of the three looped PI-FOPA variants. We additionally propose a “Gain – Loss – (Filter) – Gain – Loss” variant of a looped PI-FOPA and a Mach-Zehnder-like PI-FOPA architecture for further performance improvement.

This work comprises and extends our conference publications, which proposed idlers removal prior to the ‘Loss’ section for a penalty-free mitigation of nonlinear crosstalk [27], and compared the looped PI-FOPA variants in terms of the amplified signal BER [28] and noise figure [29], [30].

II. EXPERIMENTAL SETUP

Fig. 1(d) shows experimental setup for characterization of polarization insensitive FOPAs. It consisted of a WDM transmitter producing a set of WDM channels, one of the looped PI-FOPA variants amplifying these channels (Fig. 1(a)–(c)), and a receiver counting errors of an amplified signal. An optical spectrum analyzer (OSA) was connected to the FOPA input and output via calibrated 1% tap couplers for measurements of net gain, noise figure and nonlinear crosstalk.

The WDM transmitter produced 21×50 GHz-spaced WDM channels between 1533.5 nm (195.5 THz) and 1541.3 nm (194.5 THz) as shown at Fig. 3. The middle channel at 1537.4 nm (195 THz) was a 35 GBaud PDM-QPSK signal sourced from a Ciena transponder WaveLogic 3 with data rate of 100 Gb/s and forward error correction overhead of 29%. The remaining channels were emulated by shaping an amplified spontaneous emission (ASE) with a wavelength selective switch (WSS) to replicate the 35 GBaud PDM-QPSK channel spectral shape. The WSS combined the data channel with the emulated channels to measure the signal gain, power and BER, and blocked the data channel to measure power of noise and nonlinear crosstalk at its wavelength. All the channels were then amplified by an EDFA and passed via a variable optical attenuator (VOA) to set power per channel in the range from -25 dBm to -4 dBm. This range includes high input signal powers to evaluate the FOPA performance with high total output power, e.g., in case of a large channel count. The WDM channels’ state of polarization was not controlled.

The WDM receiver varied the signal OSNR, filtered it and measured BER at fixed received power. A fixed power ASE noise was mixed with the amplified WDM channels via a 5%

coupler to vary the received signal OSNR proportionally with its launch power. Then, a WSS filtered the 35 GBaud PDM-QPSK channel and attenuated it to set the detected signal power of -19 dBm. Finally, this channel was coherently detected by the Ciena transponder WaveLogic 3 to find the channel BER via error counting.

All examined PI-FOPA variants reused the same polarization diversity loop with minor changes (Fig. 1(a)–(c)). An input signal was injected in the loop via an optical circulator followed by a polarization beam splitter (PBS). The PBS split the input signal into two orthogonal components counter-propagating in the polarization diversity loop. Then, the PBS recombined signal components amplified in the loop and passed them to the FOPA output via the optical circulator. The minimum insertion loss from the input to the output was 5.5 dB.

The loop contained two lengths (250 m and 200 m) of HNLF, two pairs of wavelength division multiplexers, and a polarization controller (PC). The HNLF lengths had a zero-dispersion wavelength of ~ 1564 nm, a dispersion slope of ~ 84 s·m $^{-3}$ and a nonlinearity coefficient of ~ 8.2 W $^{-1}$ ·km $^{-1}$. Each pair of multiplexers coupled (MUX) and decoupled (DEMUX) signals and a pump in a respective HNLF length. Each length of HNLF was therefore a gain medium for only the signal component co-propagating with the local pump. Polarization of each pump was aligned with polarization of the corresponding signal using a PC. A PC inside the loop ensured signal components to recombine in the PBS with minimal loss.

The pumps were sourced from a single 100 kHz linewidth laser at 1564.4 nm, phase modulated with three RF tones to mitigate SBS and split in two pumps using a 50% coupler (Fig. 1(e)). The pumps were independently amplified by high power EDFAs. The pump powers were fine-tuned by variable optical attenuators (VOA) to set the 35 GBaud PDM-QPSK channel net gain of 14 ± 0.2 dB and PDG < 0.2 dB for all measurements. Pump powers in the 250 m and the 200 m HNLF lengths were in ranges of 1.9...2.4 W and 2.4...2.9 W respectively. The pump powers were increased slightly with input signal power to compensate for pump depletion and maintain the target net gain.”

The key difference between the looped PI-FOPA variants is the direction of pumps (Fig. 1, Fig. 2). In the GL and GFL variants the pumps are injected near the PBS and removed in the middle of the loop. In the LG variant the pumps are injected in the middle of the loop and removed on the PBS side of HNLF lengths. The GFL variant features an idler remover inserted between the HNLF lengths. The idler remover consisted of two C/L band splitters connected to pass the C band signals on, while removing idlers in the L band. The idler remover had insertion loss of ~ 1 dB, so pump powers were slightly higher in this scenario to deliver the same net gain.

III. RESULTS AND DISCUSSION

A. Spectral Analysis

Fig. 4 shows net gain and polarization dependent gain (PDG) of every WDM channel at input power of -25 dBm per channel for all examined FOPA variants. Net gain of all channels was found using optical power spectra measured at the input and the

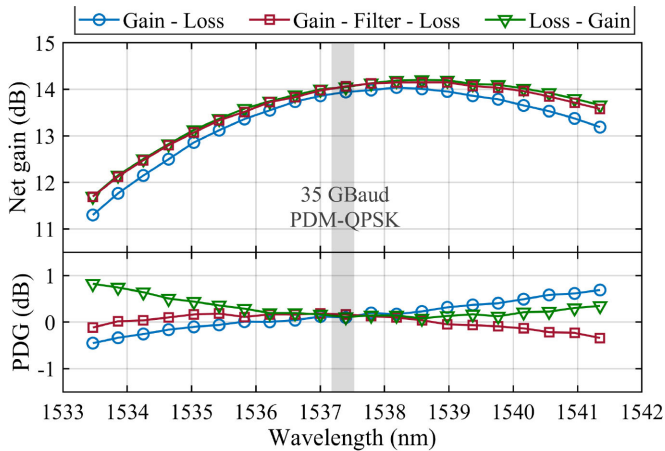


Fig. 4. Small signal net gain and polarization dependent gain (PDG) for every channel and FOPA variant. The 35 GBaud PDM-QPSK signal band is highlighted.

output of PI-FOPA and shown at Fig. 5(a). These spectra were measured via a pair of calibrated 1% tap couplers before and after the circulator (Fig. 1(d)). The PDG of all channels was found using the optical power spectra of the two signal components at the input and the output of the loop. They were measured via a pair of calibrated bidirectional 1% tap couplers connected to the PBS in the loop (Fig. 1(a)–(c)). Then, the gain for each signal component was derived, and PDG found as a difference between the signal components' gain.

Net gain of 12.8 ± 1.5 dB and PDG < 0.8 dB were observed across 21 WDM channels spanning over 8 nm. Gain spectra of each variant are sufficiently close to compare them fairly. The PDG could be improved by optimizing pump wavelengths and/or by employing gain fibers of equal length. The bandwidth occupied by WDM channels could be higher if the channels were extended towards longer wavelengths. However, gain bandwidth and PDG are not the key figures of merit for this work, so further we focus on evaluation of noise figure and nonlinear impairments in the looped PI-FOPA variants.

Fig. 5 shows comparison of optical power spectra at the output of each examined FOPA variant as input power per channel is varied from -25 dBm to -5 dBm. This corresponds to the total output signal power ranging from 2 dBm to 22 dBm. The middle channel was removed by the transmitter WSS (Fig. 1(d)) to evaluate the in-band nonlinear crosstalk. The combined power of noise and nonlinear crosstalk is highest at the middle channel in most cases, and it is only slightly lower at the signal band edges. Therefore, the middle channel is sufficiently representative to be used for further evaluation of the variants' performance. Fig. 5 shows once again that output optical spectra of all examined FOPA variants consistently overlap at frequencies where WDM channels are present, so these spectra can be used for a fair comparison of the FOPA variants.

In the linear power regime, e.g., with -25 dBm input signal power per channel, there are no signs of nonlinear crosstalk products in all FOPA variants (Fig. 5(a)). The GL and GFL variants lead to identical optical power spectra in this case, but the LG variant produces a much higher noise level.

Fig. 5(b) shows the output optical spectrum for input signal power per channel of -15 dBm, about the highest power level expected at the end of a typical fiber span. There is only residual evidence of nonlinear crosstalk, in the GL and GFL variants, in the form of a ripple around the signal band. The combined power of spontaneous noise and nonlinear interference has therefore increased in the GFL and GL variants and became 0.5 dB and 1.5 dB higher than that of the LG variant respectively.

Fig. 5(c) shows the output optical spectrum for uncharacteristically high input signal power per channel of -5 dBm and the output signal power substantially above the optimum launch power for typical optical links (~ 0 dBm). In this case significant nonlinear crosstalk products are generated in all FOPA variants, whereas the GL variant leads to the highest nonlinear crosstalk power of all. Although nonlinear interference after the GFL variant is very high too, it is ~ 4.5 dB lower than in the GL variant due to the nonlinear crosstalk mitigation by a filter. The LG variant provides a further reduction of nonlinear crosstalk by ~ 12 dB.

Overall, the GL and the GFL variants has much lower linear noise power than the LG at typical input signal power levels but suffer from much higher nonlinear crosstalk power than the LG at high input signal power. The GFL allows for as good performance as GL at low signal power and better performance than the GL at high signal power because of the filter. Next section provides a detailed comparison in terms of nonlinear crosstalk, noise figure and signal performance.

B. OSNR, Noise Figure and Bit Error Rate

In this subsection the PI-FOPA variants are characterized in terms of OSNR, noise figure and bit error rate as a function of the total output power of the WDM channels. The results are presented against the total output power because it is one of the key PI-FOPA figures of merit as its performance is often limited by nonlinear crosstalk.

Fig. 6 shows example optical spectra at the FOPA input and output for measurements of OSNR and noise figure. First, the input S_{input} and output S_{output} signal powers were measured at the central channel frequency. Second, the central channel was removed by the transmitter WSS to measure the combined power of noise and nonlinear crosstalk at the same frequency at the FOPA input (N_{input}) and output (N_{output}). The OSNR and noise figure measurements therefore accounted for a combined impact of linear noise and nonlinear crosstalk both having a Gaussian distribution in multichannel systems [31]. Then, the output signal OSNR and the FOPA noise figure were found using equations (1) and (2) [32], where G is the signal gain given by (3), h is the Planck's constant, $\nu = 195$ THz is the central channel frequency, and $B = 19$ GHz is the OSA resolution bandwidth. Fig. 6 shows that removing a channel slightly reduces the nonlinear crosstalk level by ~ 0.5 dB at the edges of the signal band. We therefore estimate that overall noise figure and OSNR measurement error was less than 1 dB.

$$OSNR_{output} = \frac{S_{output} - N_{output}}{N_{output}} \quad (1)$$

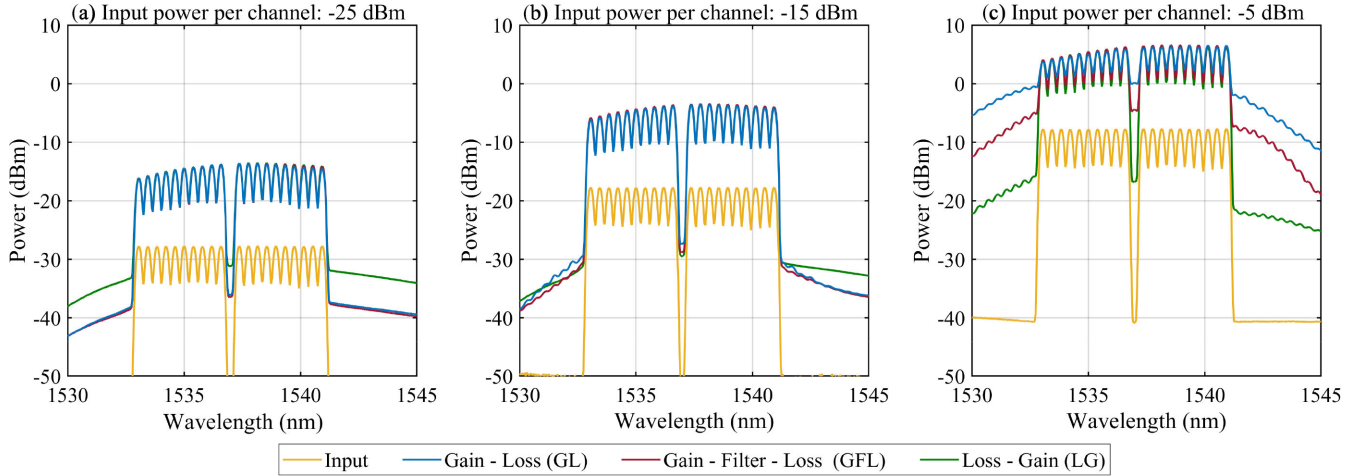


Fig. 5. Optical spectra at the input and output of each FOPA variant show power of noise and nonlinear crosstalk for a range of input signal powers. The middle channel was removed by the transmitter WSS to evaluate the in-band nonlinear crosstalk.

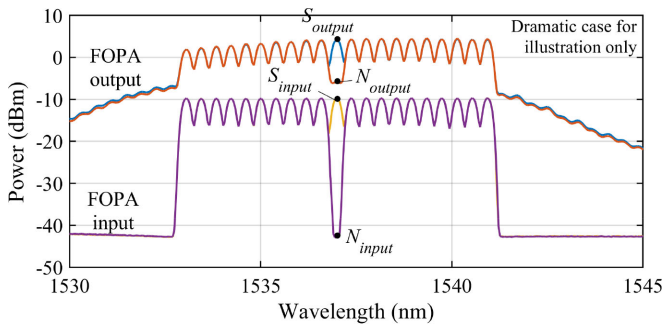


Fig. 6. Example optical power spectra at the input and the output of FOPA with and without the middle channel for OSNR and noise figure measurements. The very high nonlinear crosstalk case is shown for illustration purpose.

$$NF = \frac{N_{output}}{Gh\nu B} + \frac{1}{G} - \frac{N_{input}}{h\nu B} \quad (2)$$

$$G = \frac{S_{output} - N_{output}}{S_{input} - N_{input}} \quad (3)$$

Fig. 7 shows OSNR at the central channel versus the total power of WDM channels at the output of every FOPA configuration. The OSNR was calculated using (1) and accounted for both linear noise and nonlinear crosstalk. The OSNR was defined by linear noise at low signal power and by nonlinear crosstalk at high signal power (Fig. 5).

At low signal power the OSNR improved by 1 dB per 1 dB of signal power for all examined FOPA variants which indicates the linear operation regime. The OSNR measurements at low signal power show that the GL and the GFL variants allow for ~ 5 dB lower linear noise power than the LG variant (Fig. 7). We attribute up to 3 dB OSNR penalty to an additional signal attenuation before the gain section in the LG variant. We suggest a further penalty might be caused by aggravation of backscattering and reflections in the LG variant. A small 0.5 dB advantage of the GFL over the GL variant in the linear regime might be a measurement error, but its consistency might as well indicate a

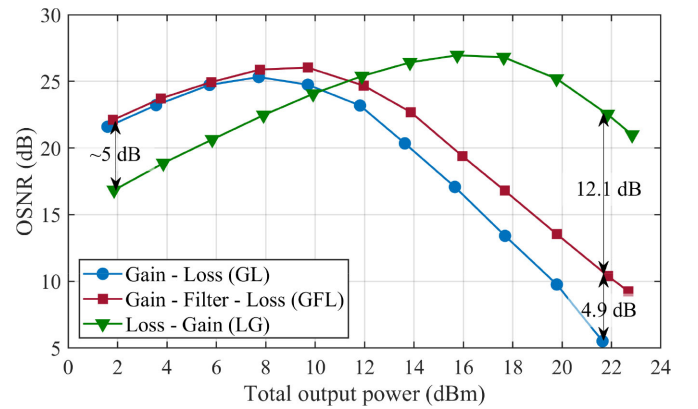


Fig. 7. OSNR of the middle channel shown as a function of total WDM channels power at the output of each FOPA variant. The OSNR shows the signal to linear noise ratio at low power and the signal to nonlinear crosstalk ratio at high power.

noise reduction in the loop due to early removal of idlers. For example, backscattering and reflections can contribute to noise of counter-propagating signals.

At high signal power the OSNR decreased by 1.8 dB per 1 dB of signal power for all examined FOPA variants which indicates operation limited by nonlinear effects. The OSNR measurements show that the LG variant mitigates nonlinear crosstalk by 12 dB and 17 dB as compared to the GFL and the LG variants respectively (Fig. 7). This implies that up to 98% of nonlinear crosstalk power in the GL variant is generated in the ‘Loss’ section. The nonlinear crosstalk power difference of 5 dB between the GL and the GFL variants means the idler removal before the ‘Loss’ section has decreased the overall nonlinear crosstalk power by a factor of ~ 3 . This implies that about 2/3 of nonlinear crosstalk power produced in the ‘Loss’ section involved idlers, which agrees with nonlinear crosstalk analysis in [34].

Overall, the LG variant has allowed for the highest OSNR of 27 dB outperforming the GFL and the GL by 1 dB and 1.7 dB respectively. Importantly, the LG variant superiority and the GL

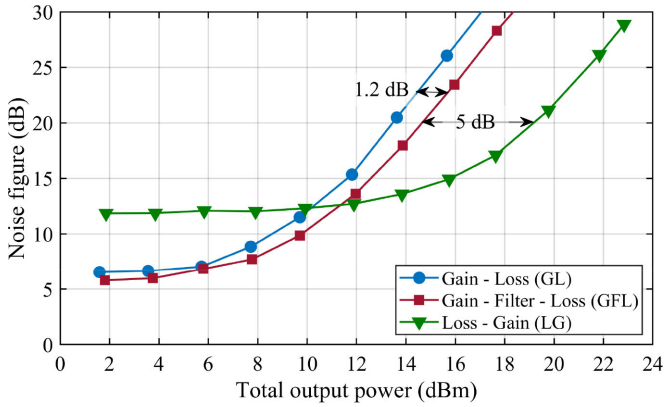


Fig. 8. Noise figure at the middle channel shown as a function of total WDM channels power at the output of each FOPA variant.

variant inferiority in terms of the peak OSNR is likely to remain unless the looped PI-FOPA is modified significantly because most system improvements affect all variants equally. Moreover, the LG variant advantage can be further improved if the 5 dB linear noise penalty is reduced.

Fig. 8 shows the noise figure measured at the central channel frequency for each looped PI-FOPA variant as the input signal power was varied. The minimum noise figure of 5.8 dB and 6.5 dB was measured for GFL and GL variants respectively when the total output power was 2 dBm. The minimum noise figure was mostly comprised of the 3 dB limit for phase-insensitive amplifier and the ~ 2 dB penalty caused by the insertion loss between the PI-FOPA input and the gain fiber [25]. The LG variant had a minimum noise figure of 11.9 dB, which is >5 dB more than the GL and the GFL variants. Although insertion loss preceding the gain fiber was as high as ~ 4 dB in the LG variant, it is 5 dB short of causing ~ 12 dB noise figure. We suggest backscattering and reflections could be an additional major source of linear noise in the LG variant.

Noise figure of all looped PI-FOPA variants increased by up to 2.8 dB per 1 dB of signal power when nonlinear crosstalk power exceeded linear noise power (Fig. 8). This means the nonlinear crosstalk power scaled with the output signal power P as $\sim P^{2.8}$ which is close to the theoretically predicted $\sim P^3$ for the second order nonlinear crosstalk dominating in the center of the signal band [34]. The noise figure of the GL variant reached 7 dB at the output signal power of 6 dBm and quickly grew with further signal power increase. The GFL variant allowed for ~ 1.2 dB higher output signal power than the GL variant for the same noise figure due to an improved nonlinear crosstalk tolerance. The LG variant demonstrated a further nonlinear crosstalk tolerance improvement by 5 dB as compared to the GFL variant. The LG variant has consequently showed the lowest noise figure of all looped PI-FOPA variants for the output signal power above 12 dBm. Emergence of nonlinear crosstalk at such a moderate signal power was due to employment of long (≥ 200 m) gain fibers [35].

Although the noise figure measurement performed in optical domain does not account for some impairments intrinsic

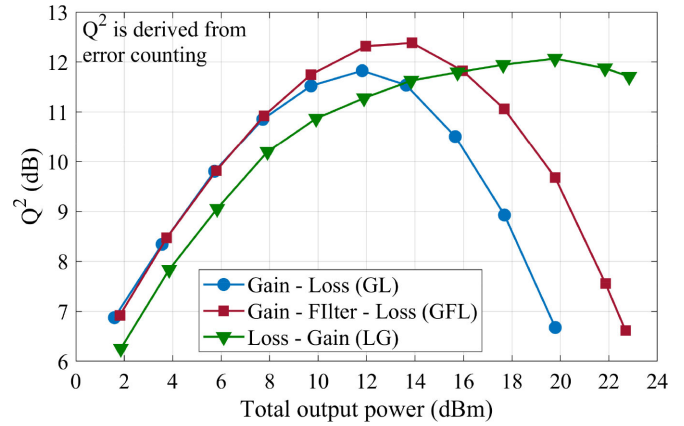


Fig. 9. Q^2 of the middle (35 GBaud PDM-QPSK) channel derived from BER and shown as a function of the total WDM channels power at the output of each FOPA variant.

to channel, e.g., intra-channel nonlinear impairments, it does account for the key sources of signal degradation: linear noise and inter-channel nonlinear impairments (nonlinear crosstalk). Thus, inter-channel nonlinear impairments dominate over the intra-channel ones for large channel counts (essentially >10) [31]. Therefore, the noise figure measurements performed here allow to analyze the trade-off between linear and nonlinear performance, whilst the BER measurements provide a complete characterization of the looped PI-FOPA variants.

$$Q^2 \text{ (dB)} = 20 \times \log_{10} \left[\sqrt{2} \times \text{erfc}^{-1} (2 \times \text{BER}) \right] \quad (4)$$

Fig. 9 shows Q^2 of the 35 GBaud PDM-QPSK channel derived from counting errors using equation (4) [36]. The GL and the GFL variants demonstrated the same Q^2 for total output signal power up to 8 dBm. A further signal power increase has invoked more nonlinear crosstalk in the GL than in the GFL, so the GFL variant has allowed for ~ 1 dB higher Q^2 peak than the GL. This agrees well with the OSNR and noise figure measurements. Although the LG variant had ~ 1 dB lower Q^2 than the other two variants at low signal power, the LG variant was superior for output signal power >16 dBm. It is remarkable the LG variant has not achieved the best Q^2 of all variants (Fig. 9) despite having achieved the best OSNR (Fig. 7). It might indicate that, in the case of the LG variant, the OSNR and noise figure measurements have not captured some of the degradation phenomena which may disappear when removing a channel as described in the measurement procedure. Such phenomena might include backscattering or reflections (e.g., from bad splices between HNLF and SMF) which impact could have been exaggerated in the LG variant due its specific location, direction of pumps, etc. Nevertheless, the LG variant has allowed for operable $Q^2 > 11.7$ dB (BER of 6×10^{-5}) up to the maximum tested output signal power of 23 dBm.

The looped FOPA variants examined in this work are polarization insensitive because they can provide polarization dependent gain close to 0 dB (Fig. 4) and can amplify without much degradation polarization-multiplexed signals, in which the state of

polarization changes rapidly on a symbol rate timescale. Indeed, the maximum BER of 10^{-5} ($Q^2 = 12.4$ dB) limited by nonlinear crosstalk has been achieved in this experiment (Fig. 9), while [21] demonstrates that polarization dependent gain must be <0.2 dB to achieve such a BER. Although the PI-FOPA variants employ three polarization controllers (PCs), these PCs were only used to compensate for slow drifts within FOPA. This is different from polarization sensitive FOPAs which employ PCs to adjust for input signal polarization change and therefore cannot amplify polarization multiplexed signals due to very fast (tens of GHz) evolution of their state of polarization. The difference is made by a PBS in the PI-FOPA loop which produces signal components with fixed or slowly drifting states of polarization depending on the fibers used. Therefore, the PCs employed by the examined PI-FOPA can be either automated using a feedback from power monitors [33] or removed if polarization-maintaining fibers and components are used in the loop [19].

C. Potential Applications

Looped polarization-insensitive FOPAs provide a platform to exploit the most prominent achievements of single polarization parametric amplification, such as multiband high gain amplification [4], [6], phase-sensitive amplification [9]–[11], etc. Looped PI-FOPAs can therefore be implemented for any applications envisaged for FOPAs.

Noise figure and the maximum output power are the key parameters for most application scenarios. Their values obtained in this paper allow to assess applicability of each looped PI-FOPA variant, but they also can be significantly improved in a few ways. We realistically expect the minimum noise figure <5 dB after optimization of components and splices insertion loss. Besides, every gain fiber length L reduction by a factor of 2 allows to increase the output signal power P by ~ 2 dB whilst keeping the same nonlinear crosstalk power scaling as $\sim P^3 L^2$ [34], [35]. Therefore, an employment of 25 m long gain fibers [3] instead of 200 m and 250 m lengths would allow for >6 dB higher output signal power without aggravating nonlinear crosstalk. These improvements will enable the GFL variant to deliver a noise figure <6 dB with total output signal power >13 dBm, and the LG variant to remain operable with total output signal power >29 dBm. The allowed output signal power is expected to be even higher if signals are distributed over wider bandwidth than in this experiment.

The GL and the GFL variants can be applied when low noise figure is required, because they have demonstrated an EDFA-like noise figure of ~ 6 dB with potential for further improvement. The GFL additionally allows for higher output power than the GL, therefore the GFL is the most suitable looped PI-FOPA variant for most applications, e.g., multi-span broadband communications. The GL variant is however the most suitable for prospective polarization-insensitive phase-sensitive amplifiers because it allows to keep signal copies unlike the GFL variant.

The LG variant is for high output signal power applications because it has allowed for output signal power of 23 dBm in this experiment and has potential for operation with output signal

power of ~ 1 W if 25 m long gain fibers are implemented. Although we have not achieved an EDFA-like noise figure for the LG variant, it can be used in links where noise figure is not the key parameter, e.g., single-amplifier links. Thus, the LG variant is the most suitable looped PI-FOPA variant for an extended reach PON, because it allows for operation with the highest output signal power and consequently for the highest splitter loss [37]. In addition, the LG variant has the potential to provide the highest Q^2 of all variants upon mitigation of signal penalties that appear related with backscattering and/or reflections.

High output power operation with low noise figure might require more advanced PI-FOPA architectures. An employment of four gain fiber lengths arranged as “Gain – Loss – (Filter) – Gain – Loss” [26] splits gain between two gain sections, reduces gain fibers’ lengths, and therefore mitigates nonlinear crosstalk occurring in the final ‘Loss’ section. This can significantly improve the nonlinear tolerance of the GL and the GFL variants. Alternatively, the loop can be replaced with the Mach-Zehnder architecture similar to LiNbO₃-based polarization-insensitive optical parametric amplifiers [38]. This architecture can have a noise figure of the GL variant and the nonlinearity tolerance of the LG variant simultaneously. It therefore has a potential to satisfy requirements of the most demanding application scenarios by delivering noise figure less than 6 dB with output signal power more than 29 dBm if the improvements suggested above are implemented.

IV. CONCLUSION

We have examined three variants of looped polarization insensitive FOPA: “Gain – Loss” (GL), “Gain – Filter – Loss” (GFL) and “Loss – Gain” (LG), when amplifying 21 WDM channels including a 35 GBaud PDM-QPSK signal. The GL variant has demonstrated a noise figure of 6.5 dB, but its susceptibility to nonlinear crosstalk caused a significant noise figure degradation at output power over 6 dBm. The GFL variant has achieved an EDFA-like noise figure of 5.8 dB and reduced power of nonlinear crosstalk by 4.9 dB as compared to the GL variant. It therefore allowed for low noise figure operation for output signal power up to ~ 7 dBm. The LG variant has further reduced the nonlinear crosstalk power by 12 dB but had the minimum noise figure of 11.9 dB. Although the GFL variant has allowed for the highest peak Q^2 of all variants, the LG variant was superior for output signal power >16 dBm and was operable with signal BER of 6×10^{-5} at the maximum tested output signal power of 23 dBm.

We have suggested several ways to improve performance of looped polarization insensitive FOPAs, e.g., employment of four unidirectional gain fibers and Mach-Zehnder-like architecture instead of a loop. We consequently justified the polarization insensitive FOPA potential for noise figure <6 dB at output signal power up to 29 dBm, which can satisfy the most demanding requirements of modern optical communication systems. We therefore envisage the discussed polarization insensitive FOPA variants to realize FOPA’s potential for wavelength unconstrained operation, ultra-wide gain bandwidth, instantaneous

response time and phase-sensitive amplification in commercial links.

ACKNOWLEDGMENT

We thank Dr Charles Laperle of Ciena for provision of a transponder and related support. We thank the AIPT technician Ms Swaroopa Mucheli-Sudhakar for continuous assistance in the lab. The data reported in this paper is available as part of the U.K. EPSRC open access policy at <https://doi.org/10.17036/researchdata.aston.ac.uk.00000506>.

REFERENCES

- [1] A. Ferrari *et al.*, "Assessment on the achievable throughput of multi-band ITU-T G.652.D fiber transmission systems," in *J. Lightw. Technol.*, vol. 38, no. 16, pp. 4279–4291, Aug. 2020, doi: [10.1109/JLT.2020.2989620](https://doi.org/10.1109/JLT.2020.2989620).
- [2] M. E. Marhic, N. Kagi, T.-K. Chiang, and L. G. Kazovsky, "Broadband fiber optical parametric amplifiers," *Opt. Lett.*, vol. 21, no. 8, pp. 573–575, Apr. 1996, doi: [10.1364/OL.21.000573](https://doi.org/10.1364/OL.21.000573).
- [3] V. Gordienko, M. F. C. Stephens, A. E. El-Taher, and N. J. Doran, "Ultra-flat wideband single-pump Raman-enhanced parametric amplification," *Opt. Exp.*, vol. 25, no. 5, pp. 4810–4818, Mar. 2017, doi: [10.1364/OE.25.004810](https://doi.org/10.1364/OE.25.004810).
- [4] M. E. Marhic, K. K.-Y. Wong, and L. G. Kazovsky, "Wide-band tuning of the gain spectra of one-pump fiber optical parametric amplifiers," in *IEEE J. Sel. Topics Quantum Electron.*, vol. 10, no. 5, pp. 1133–1141, Sep./Oct. 2004, doi: [10.1109/JSTQE.2004.835298](https://doi.org/10.1109/JSTQE.2004.835298).
- [5] C. Fourcade-Dutin *et al.*, "12 THz flat gain fiber optical parametric amplifiers with dispersion varying fibers," *Opt. Exp.*, vol. 23, no. 8, pp. 10103–10110, Apr. 2015, doi: [10.1364/OE.23.010103](https://doi.org/10.1364/OE.23.010103).
- [6] J. M. C. Boggio, S. Moro, E. Myslivets, J. R. Windmiller, N. Alic, and S. Radic, "155-nm continuous-wave two-pump parametric amplification," *IEEE Photon. Technol. Lett.*, vol. 21, no. 10, pp. 612–614, May 2009, doi: [10.1109/LPT.2009.2015276](https://doi.org/10.1109/LPT.2009.2015276).
- [7] M. Jamshidifar, A. Vedadi, and M. E. Marhic, "Continuous-wave one-pump fiber optical parametric amplifier with 270 nm gain bandwidth," in *Proc. 35th Eur. Conf. Opt. Commun.*, Vienna, Austria, 2009, pp. 1–2.
- [8] M. Vasilyev, "Distributed phase-sensitive amplification," *Opt. Exp.*, vol. 13, no. 19, pp. 7563–7571, Sep. 2005.
- [9] V. Gordienko, F. Ferreira, J. R. Lamb, Á. Szabó, and N. Doran, "Phase-sensitive amplification of 11 WDM channels across bandwidth of 8 nm in a fibre optic parametric amplifier," in *Proc. Eur. Conf. Opt. Commun.*, Brussels, Belgium, 2020, pp. 1–4, doi: [10.1109/ECOC48923.2020.9333194](https://doi.org/10.1109/ECOC48923.2020.9333194).
- [10] R. Kakarla, J. Schröder, and P. A. Andrekson, "One photon-per-bit receiver using near-noiseless phase-sensitive amplification," *Light: Sci. Appl.*, vol. 9, no. 153, pp. 1–7, Sep. 2020, doi: [10.1038/s41377-020-00389-2](https://doi.org/10.1038/s41377-020-00389-2).
- [11] S. L. I. Olsson, H. Eliasson, E. Astra, M. Karlsson, and P. A. Andrekson, "Long-haul optical transmission link using low-noise phase-sensitive amplifiers," *Nature Commun.*, vol. 9, Jun. 2018, Art. no. 2513, doi: [10.1038/s41467-018-04956-5](https://doi.org/10.1038/s41467-018-04956-5).
- [12] R. W. Boyd, "The intensity-dependent refractive index," in *Nonlinear Optics*, 3rd ed., Acad. press, 2008, ch. 4, sec. 4.1. pp. 207–211.
- [13] C. B. Gaur, F. Ferreira, V. Gordienko, V. Ribeiro, Á. D. Szabó, and N. J. Doran, "Experimental comparison of fiber optic parametric, Raman and erbium amplifiers for burst traffic for extended reach PONs," *Opt. Exp.*, vol. 28, no. 13, pp. 19362–19373, Jun. 2020, doi: [10.1364/OE.394379](https://doi.org/10.1364/OE.394379).
- [14] T. Kobayashi *et al.*, "Wide-band inline-amplified WDM transmission using PPLN-based optical parametric amplifier," *J. Lightw. Technol.*, vol. 39, no. 3, pp. 787–794, Feb. 2021, doi: [10.1109/JLT.2020.3039192](https://doi.org/10.1109/JLT.2020.3039192).
- [15] S. Shimizu *et al.*, "Non-degenerate phase-sensitive amplification scheme using digital dispersion pre-equalization for unrepeatable transmission," *Opt. Exp.*, vol. 29, no. 6, pp. 8451–8461, Mar. 2021, doi: [10.1364/OE.419782](https://doi.org/10.1364/OE.419782).
- [16] K. K. Y. Wong, M. E. Marhic, K. Uesaka, and L. G. Kazovsky, "Polarization-independent two-pump fiber optical parametric amplifier," *IEEE Photon. Technol. Lett.*, vol. 14, no. 7, pp. 911–913, Jul. 2002, doi: [10.1109/LPT.2002.1012382](https://doi.org/10.1109/LPT.2002.1012382).
- [17] H. Hu *et al.*, "Parametric amplification, wavelength conversion, and phase conjugation of a 2.048-Tbit/s WDM PDM 16-QAM signal," *J. Lightw. Technol.*, vol. 33, no. 7, pp. 1286–1291, Apr. 2015, doi: [10.1109/JLT.2014.2370038](https://doi.org/10.1109/JLT.2014.2370038).
- [18] M. E. Marhic, K. K. Y. Wong, and L. G. Kazovsky, "Fiber optical parametric amplifiers with linearly or circularly polarized waves," *J. Opt. Soc. Amer. B*, vol. 20, no. 12, pp. 2425–2433, Dec. 2003, doi: [10.1364/JOSAB.20.002425](https://doi.org/10.1364/JOSAB.20.002425).
- [19] S. Takasaka and R. Sugizaki, "Polarization insensitive fiber optical parametric amplifier using a SBS suppressed diversity loop," in *Proc. Opt. Fiber Commun. Conf.*, 2016, Paper M3D.4, doi: [10.1364/OFC.2016.M3D.4](https://doi.org/10.1364/OFC.2016.M3D.4).
- [20] M. Jazayerifar *et al.*, "Impact of Brillouin backscattering on signal distortions in single-fiber diversity loop based polarization-insensitive FOPAs," *J. Lightw. Technol.*, vol. 35, no. 19, pp. 4137–4144, Oct. 2017, doi: [10.1109/JLT.2017.2735190](https://doi.org/10.1109/JLT.2017.2735190).
- [21] M. F. C. Stephens, V. Gordienko, and N. J. Doran, "20 dB net-gain polarization-insensitive fiber optical parametric amplifier with >2 THz bandwidth," in *Opt. Exp.*, vol. 25, no. 9, pp. 10597–10609, May 2017, doi: [10.1364/OE.25.010597](https://doi.org/10.1364/OE.25.010597).
- [22] M. F. C. Stephens, M. Tan, V. Gordienko, P. Harper, and N. J. Doran, "In-line and cascaded DWDM transmission using a 15dB net-gain polarization-insensitive fiber optical parametric amplifier," *Opt. Exp.*, vol. 25, no. 20, pp. 24312–24325, Oct. 2017, doi: [10.1364/OE.25.024312](https://doi.org/10.1364/OE.25.024312).
- [23] V. Gordienko, M. Stephens, and N. Doran, "Towards wide-bandwidth ultra-flat FOPAs," in *Proc. 19th Int. Conf. Transparent Opt. Netw.*, 2017, Paper We.D5.1, doi: [10.1109/ICTON.2017.8025079](https://doi.org/10.1109/ICTON.2017.8025079).
- [24] H. Friis, "Noise figures of radio receivers," in *Proc. I.R.E.*, Jul. 1944, vol. 32, no. 7, pp. 419–422, doi: [10.1109/JRPROC.1944.232049](https://doi.org/10.1109/JRPROC.1944.232049).
- [25] E. Desurvire, "Fundamentals of noise in optical fiber amplifiers," in *Erbium-Doped Fiber Amplifiers*, Hoboken, NJ, USA: Wiley, 2002, sec. 2.5, pp. 114–121.
- [26] M. F. C. Stephens, V. Gordienko, and N. J. Doran, "Reduced crosstalk, polarization insensitive fiber optical parametric amplifier (PI FOPA) for WDM applications," in *Proc. Opt. Fiber Commun. Conf. Expo.*, 2018, Paper W3D.4.
- [27] V. Gordienko, F. M. Ferreira, V. Ribeiro, and N. Doran, "Suppression of nonlinear crosstalk in a polarization insensitive FOPA by mid-stage idler removal," in *Proc. Opt. Fiber Commun. Conf.*, 2019, Paper M4C.4.
- [28] V. Gordienko *et al.*, "Characterisation of novel polarisation-insensitive configurations of fibre optical parametric amplifiers," in *Proc. 45th Eur. Conf. Opt. Commun. (ECOC 2019)*, Dublin, Ireland, 2019, Paper Th.1.C.5, doi: [10.1049/cp.2019.0978](https://doi.org/10.1049/cp.2019.0978).
- [29] V. Gordienko *et al.*, "Noise figure evaluation of polarization-insensitive single-pump fiber optical parametric amplifiers," in *Proc. Opt. Fiber Commun. Conf.*, 2020, Paper W4B.4, doi: [10.1364/OFC.2020.W4B.4](https://doi.org/10.1364/OFC.2020.W4B.4).
- [30] V. Gordienko, F. Ferreira, C. Laperle, M. O'Sullivan, K. Roberts, and N. Doran, "Polarisation-insensitive fibre optic parametric amplifiers for applications in modern communication networks," in *Proc. 22nd Int. Conf. Trans. Opt. Netw. (ICTON 2020)*, Bari, Italy, Paper Th.A6.2, doi: [10.1109/ICTON51198.2020.9203518](https://doi.org/10.1109/ICTON51198.2020.9203518).
- [31] Á. D. Szabó, V. Ribeiro, V. Gordienko, F. Ferreira, C. Gaur, and N. Doran, "Verification of signal-to-crosstalk measurements for WDM fiber optical parametric amplifiers," in *Proc. Conf. Lasers Electro-Opt.*, 2020, Paper JTu2E.1.
- [32] D. M. Baney, P. Gallion, and R. S. Tucker, "Theory and measurement techniques for the noise figure of optical amplifiers," *Opt. Fiber Technol.*, vol. 6, no. 2, pp. 122–154, Apr. 2000, doi: [10.1006/ofte.2000.0327](https://doi.org/10.1006/ofte.2000.0327).
- [33] V. Gordienko, C. B. Gaur, F. Bessin, I. D. Phillips, and N. J. Doran, "Robust polarization-insensitive C & L band FOPA with >17dB gain for both WDM and bursty traffic," in *Proc. Opt. Fiber Commun. Conf.*, 2021, Paper M5B.4.
- [34] V. Gordienko, M. A. Z. Al-Khateeb, F. M. Ferreira, A. D. Ellis, and N. J. Doran, "Unwanted four-wave mixing in fibre optical parametric amplifiers," in *Proc. 21st Int. Conf. Transparent Opt. Netw.*, 2019, Paper Fr.C4.4, doi: [10.1109/ICTON.2019.8840198](https://doi.org/10.1109/ICTON.2019.8840198).
- [35] M. Jamshidifar, A. Vedadi, and M. E. Marhic, "Reduction of four-wave-mixing crosstalk in a short fiber-optical parametric amplifier," *IEEE Photon. Technol. Lett.*, vol. 21, no. 17, pp. 1244–1246, Sep. 2009, doi: [10.1109/LPT.2009.2025051](https://doi.org/10.1109/LPT.2009.2025051).
- [36] "Test methods applicable to optical fibre submarine cable systems," Rec. ITU-T G.976, Int. Telecommun. Union, May 2014.
- [37] C. B. Gaur, V. Gordienko, F. Bessin, and N. J. Doran, "Dual-band amplification of downstream L-band and upstream C-band signals by FOPA in extended reach PON," in *Eur. Conf. on Opt. Commun. (ECOC)*, Brussels, Belgium, 2020, Paper Th2A-5, doi: [10.1109/ECOC48923.2020.9333421](https://doi.org/10.1109/ECOC48923.2020.9333421).
- [38] T. Kobayashi *et al.*, "Wide-Band inline-amplified WDM transmission using PPLN-Based optical parametric amplifier," *J. Lightw. Technol.*, vol. 39, no. 3, pp. 787–794, Feb. 2021, doi: [10.1109/JLT.2020.3039192](https://doi.org/10.1109/JLT.2020.3039192).

Vladimir Gordienko received the B.Eng. degree in optical technology from Bauman Moscow State Technical University, Moscow, Russia, in 2010, the dual M.Sc. degrees from Aston University, Birmingham, U.K. and Sant'Anna School of Advanced Studies, Pisa, Italy, in 2013, and the Ph.D. degree in broadband fiber optical parametric amplifiers from Aston University, in 2018. He then joined EPSRC funded projects UPON and FPA-ROCS and worked on delivery of two industrially funded projects. He is currently a Research Fellow leading teams working on fiber optical parametric amplifiers and optical wavelength converters with Aston University. He has authored or coauthored about 30 papers and provided various breakthroughs and novel concepts in areas of ultra-wide, Raman-assisted, polarisation insensitive, and phase-sensitive operation of fiber optical parametric amplifiers. He was awarded a scholarship for Erasmus Mundus program MAPNET.

Filipe M. Ferreira (Senior Member, IEEE) received the Ph.D. degree in electrical and computer engineering from the University of Coimbra, Coimbra, Portugal, in 2014, for his work on high-capacity optical transmission over multipath fibres. During this time, he was a Research Engineer with Nokia Siemens Networks leading various research advances in mode-division multiplexing under the EU-FP7 project MODEGAP. During this period, he advanced the understanding of the interplay between linear and nonlinear impairments in multimode fibres and its impact on the achievable transmission capacity. In 2019, Filipe joined the EPSRC TRANSNET programme, University College London, London, U.K., as a Senior Research Fellow to work in developing intelligent transceivers capable for better approaching the Shannon limit. In 2020, he was awarded a UKRI Future Leaders Fellowship to work on exploiting massive spatial parallelism in multimode optical fibres by merging spatial light modulation with machine learning. He was then awarded a Marie Skłodowska-Curie Fellowship to continue his research with Aston University, Birmingham, U.K.

Chandra B. Gaur received the B.Eng. degree in electronics and communication from Visvesvaraya Technological University, Karnataka, India in 2008 and the M.Sc. degree in photonics from the University of Strathclyde, Glasgow, U.K., in 2011. He is currently working toward the Ph.D. degree in optical communication from Aston University, Birmingham, U.K. He was with multiple organizations on optical fiber projects. His research interests include optical fiber parametric amplifiers, optically amplified passive optical networks, all optical wavelength conversion, and phase sensitive amplification.

Nick J. Doran was a Research Leader in optical communications and nonlinear fiber optics for more than 40 years. He has led advanced research teams in BT Labs, Aston University, Marconi, Swansea University and lately back at Aston. He has authored or coauthored more than 300 papers on optical transmission and devices and is an established authority on nonlinear fiber transmission and devices including amplifiers and switches. He has more than 20 patents and is an acknowledged world leader in the subject of soliton transmission and processing. He pioneered the concept of dispersion managed solitons and invented the extensively used nonlinear optical loop mirror which currently has more than 1000 citations. He co-founded the Photonics Research Group (currently AiPT), Aston University 1991 with Prof I Bennion. During this first time with Aston his research was extensively funded by a series of major EPSRC grants with significant industrial support from key industrial operators including BT, KDDI, and Marconi.